PHYSICAL REVIEW B VOLUME 16, NUMBER 12 15 DECEMBER 1977

Resonant first- and second-order Raman scattering in gray tin

M. Iliev,* M. Sinyukov,† and M. Cardona
Max-Planck-Institut für Festkörperforschung, 7 Stuttgart 80, Federal Republic of Germany
(Received 8 August 1977)

The first- and second-order Raman scattering by phonons has been investigated in α-Sn as a function of scattering photon energy. A resonant behavior of both first- and second-order processes has been found near the $E_1 + \Delta_1$ gap ($\sim$ 1.85 eV) and a resonance of the first-order process near E_2 (3.7 eV). The scattering by 2Γ (O) phonons develops a peak near resonance in a manner similar to that found for Ge and Si. The results are interpreted in terms of two- and three-band scattering processes.

I. INTRODUCTION

The first- and second-order Raman scattering (RS) in the diamond and zinc-blende structure semiconductors has received considerable attention during the recent years. In particular, the resonance behavior of the RS cross section in the neighborhood of the E_0 and E_1 gaps was studied for Ge,[1-3] Si,[4] and InSb,[5,6] using cw dye lasers and a number of ion-laser lines. The results have been interpreted in terms of deformation-potential theory[7,8] and the electron-phonon and electron–two-phonon coupling constants have been determined from these measurements. The second-order RS spectra of the above-mentioned materials have been measured for several scattering configurations, which enables the separation of two-phonon processes of different symmetry (Γ_1, Γ_{12}, and Γ'_{25}). The main features of the second-order spectra are consistent with the data of inelastic neutron scattering and of optical absorption.

Contrary to other tetrahedral semiconductors, relatively few experimental studies have been devoted to the lattice dynamics of gray tin (α-Sn). Here one should mention the works of Myers[9] and Price *et al.*[10] on inelastic neutron scattering, and the work of Buchenauer *et al.*,[11] in which the Raman frequency and its temperature dependence have been determined.

The lack of data on the Raman scattering of gray tin finds its explanation in the difficulties one faces working with this zero-gap material. Beside relatively weak scattering intensity, due to the high absorption coefficient ($\alpha > 10^5$ cm^{-1}) in the whole region where laser lines are available, considerable difficulties come from the fact that α-Sn is stable only below 13 °C. This makes practically impossible any grinding and polishing of the samples and one has to use as-grown surfaces, the latter giving rise to unwanted background originating from diffuse Rayleigh scattering. Additionally, the temperature limit restricts the maximum allowable incident laser power.

In this work, we report results of measurements of the relative cross section for first-order RS in α-Sn as a function of laser frequency in the 1.55–3.5-eV range. At low photon energies a resonance due to an intraband deformation-potential mechanism at the E_1 and $E_1 + \Delta_1$ gaps is seen. Above 2.5 eV, the cross section increases again as a result of a resonance related to the E_2 gap (3.7 eV). The second-order RS spectrum of α-Sn is relatively simple and resembles that of Ge and Si. The experimental spectra are compared with calculated two-phonon density of states[12] and the energies of several two-phonon critical points are determined. A qualitative measurement of the second-order resonance curve shows that two-band interband processes are essential in this case.

II. EXPERIMENT

The Raman experiments were made in backscattering configuration on as-grown (111) surfaces of two single crystals of α-Sn. The samples were mounted on the cooled finger of a liquid-nitrogen cryostat and the average temperature in the scattered volume was controlled by measurement of the ratio between peak areas of Stokes and anti-Stokes components (although this may lead to big uncertainties in the region of strong resonance[13]). When possible, the incident laser power was kept at 100 mW. Under these conditions, the estimated average temperature, ranged between 100 and 150 °K.

In our measurements we have used 22 discrete laser lines of a 165 Spectra Physics Ar-ion laser, a Spectra Physics 170 Kr-ion laser, and a He-Cd laser. The scattered light was analyzed with a Spex double monochromator by means of photon counting. When the resonance was studied, the scattering strengths were compared to CaF_2 in order to provide a calibration for the spectral response of the entire apparatus (the ω^4 dependence is also automatically removed by this procedure).

The absorption and reflection losses, which occur for the incident and scattered light, were also accounted for by using the experimental data for the optical constants of α-Sn, taken from the work of Hanyu.[14]

Since the second-order RS spectrum of α-Sn is quite weak and its measurement is additionally complicated by a strong background, long integration times between 100 and 600 sec/channel and spectrometer scan speed between 0.05 and 0.002 Å/sec were used. At such extreme conditions one run takes many hours and the different part of the spectrum had to be taken several times to assure against long-term drifts of the electronic system.

III. RESULTS AND DISCUSSION

A. First-order resonant scattering

The results for the resonance of the first-order RS in α-Sn between 1.55 and 3.5 eV are shown in Fig. 1. The matching of data points taken with different lasers is good. The most prominent feature is the strong decrease of the RS cross section between 1.55 and 2.5 eV. No peaks or shoulders are clearly pronounced in this region within the uncertainty of the measured RS intensity. Above 2.5 eV, the scattered intensity increases again. We have, however, only two points at higher energies and thus it is difficult to make any definite conclusions about the exact line shape of this resonance.

To discuss the results of Fig. 1 we will use the band-structure scheme of gray tin[15] and will follow the dielectrical approach developed earlier for[3]

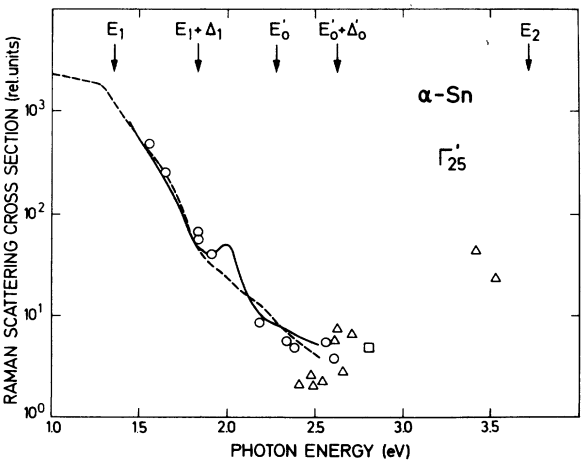

FIG. 1. Resonance in the Raman scattering of α-Sn at liquid-nitrogen temperature. The positions of the E_1, $E_1+\Delta_1$, and E_2 gaps is from Ref. 15. Curves through the points were obtained from Eq. (1) with $d^5_{1,0}=0$ (dashed) and with $d^5_{3,0}/d^5_{1,0}=-3.5$ (solid).

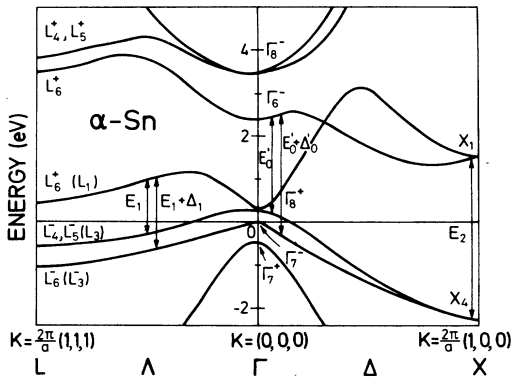

FIG. 2. Band structure of α-Sn illustrating the positions of the E_1, $E_1+\Delta_1$, E_2, $E_0'+\Delta_0$ edges.

Ge and Si.

Although α-Sn is a member of the family of tetrahedral semiconductors, its peculiar band structure (Fig. 2) makes it a semimetal. The energy gap E_0 is fixed at zero at all temperatures and pressures. The next set of gaps is the $E_1-E_1+\Delta_1$ doublet at 1.37 and 1.85 eV, respectively (at 200 °K). These gaps are attributed to transitions between spin-orbit split valence (Λ_3) and conduction (Λ_1) bands along $\langle 111\rangle$ directions. The initial and final bands are nearly parallel, thus giving rise to two-dimensional critical points in the combined electron density of states. Three other transitions are also indicated on Fig. 2. These are the doublet $E_0'-E_0'+\Delta_0'$ (2.3–2.6 eV) and E_2 (3.7 eV) which have been seen as weak and strong peaks, respectively, both in the reflectance[14,16] and electroreflectance.[15]

The quasistatic theory of the resonant RS has been already successfully applied to interpret the experimentally observed line shapes of RS cross section vs photon energy for a number of diamond and zinc-blende semiconductors.[8] In particular, it was shown that for the E_1 and $E_1+\Delta_1$ gaps that there are two main contributions to the Raman tensor, namely two-band terms due to the modulation of the gaps (Λ_3-Λ_1) by the phonons and three-band terms corresponding to the coupling by the phonon of the spin-orbit split valence bands Λ_3. The only independent component Γ_{25}' of the complex first-order Raman tensor is given by

$$d_1=\left(\frac{2\sqrt{2}}{\sqrt{3}}\frac{\chi^+-\chi^-}{\Delta_1}d^5_{3,0}+\frac{1}{2\sqrt{3}}\frac{d\chi}{d\omega}d^5_{1,0}\right)\times\left[\frac{\hbar^2}{4MN\omega_{ph}a^2}(1+n_B)\right]^{1/2} \quad (1)$$

where $d^5_{3,0}$ and $d^5_{1,0}$ are the averaged one-phonon deformation potentials, χ^+ and χ^- are the contributions to the complex scalar susceptibility χ

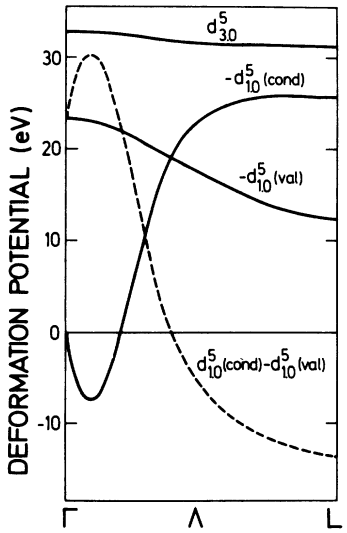

FIG. 3. Deformation potentials of the Λ_1 (conduction) and Λ_3 (valence) band edges of InSb (Ref. 17).

$=(\epsilon-1)/4\pi$ of E_1, and $E_1+\Delta_1$, respectively, a is the lattice constant, n_B the statistical factor, ω_{ph} the phonon frequency, M the average atomic mass, and N the number of unit cells per unit volume. The cross section for the first-order RS is proportional to ω^4 multiplied by the square of the expression on the right-hand side of Eq. (1).

The first term in large parentheses of Eq. (1) represents three-band contributions while the second term gives the two-band effects. The line shape and the relative weight of these two terms depends both on the spectral dependence of the complex susceptibility and the values of $d^5_{3,0}$, $d^5_{1,0}$, and Δ_1. Although the derivative $d\chi/d\omega$ should be strongly enhanced near E_1, and $E_1+\Delta_1$, the measurements on Ge and Si have demonstrated that the Raman tensor is dominated by three-band terms.

We have used Eq. (1) to calculate the theoretical dependence of the first-order RS cross section vs photon energy in the case of gray tin. For estimation of the average values of the deformation potentials, the data of pseudopotential calculations of Zeyher[17] for InSb for the variations of $d^5_{3,0}$ and $d^5_{1,0}$ along [111] were available (Fig. 3). The corresponding deformation potentials for α-Sn should be nearly the same. The dielectric constant was taken from the works of Hanyu[14] and Lindquist and Ewald[18]; the χ^+ and χ^- contributions being separated in the manner suggested by Aspnes and Cardona[19] (see Fig. 4). The two theoretical curves of Fig. 1 were obtained with $d^5_{3,0}/d^5_{1,0}=-3.5$ eV, the average value obtained from Fig. 3, (full line) and $d^5_{3,0}/d_{1,0}=\infty$ (dashed line). In the latter case, we simply neglect two-band contributions. The two curves are nearly identical and fit well the experimental points, which demonstrate the dominance of the three-band terms in the resonant RS of gray tin near E_1 gap.

Although consistent with earlier conclusions for Ge and Si, the above result differs from the data of Dreybrodt *et al.*[5] for the isoelectronic InSb. In that case, a relatively strong contribution of two-band terms has been observed in the resonance of TO phonons and the experimental points have been fitted using the values $d^5_{3,0}/d^5_{1,0}=-0.4$ and $d^5_{3,0}/d^5_{1,0}=-2.9$ for scattering from (011) and (111) surfaces, respectively. There is no reason, however, for the deformation potentials to be surface-dependent and to differ so much from the theoretically estimated ratio in the case of a (011) surface. Thus we believe that the two-band contributions in 1TO-phonon resonance near E_1 and $E_1+\Delta_1$ in InSb become important only due to sharp structure in χ, i.e., $d\chi/d\omega$ being strongly enhanced. Such sharp structure may originate from exciton transitions.[20] Thus it could depend on the surface being measured and should not be so strongly pronounced in the case of semimetallic gray tin.

In view of the good agreement between the experiments and the theoretical curve of Fig. 1, we have tried to determine the value of the deforma-

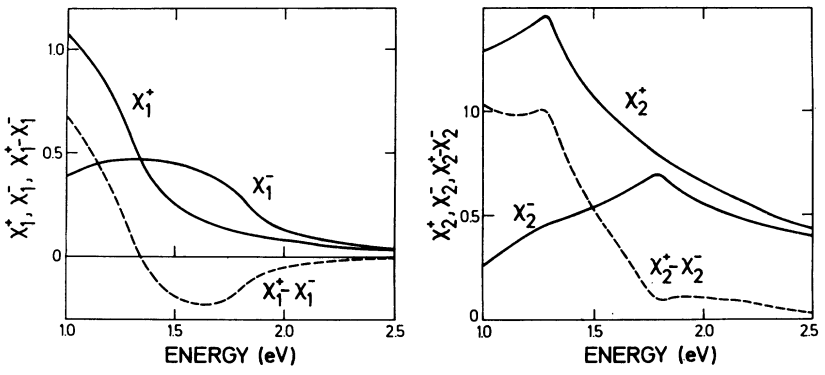

FIG. 4. Dependence of χ^+, χ^-, and $\chi^+-\chi^-$ vs photon energy of the of α-Sn obtained from the data of Ref. 14.

tion potential $d^5_{3,0}$ of Eq. (1) ($d^5_{1,0} \simeq 0$) by measuring the scattering efficiency of α-Sn at 1.92 eV with respect to that of silicon. The efficiency of silicon can be obtained from the Raman tensor P, calculated by Swanson and Maradudin[21] to be 19 Å at 1.92 eV. The excellent agreement between the dispersion of P given by these authors and that found experimentally[4] supports this value of P. The scattering efficiency S of Si is found from P with the expression[8]:

$$S = 4P^2(1+n_B)h\omega^4/a^3 M\omega_{ph}c^4 , \quad (2)$$

ω being the laser frequency and c the speed of light. The scattering efficiency of α-Sn near $E_1 + \Delta_1$ is obtained by replacing Eq. (1) into:

$$S = d_1^2\omega^4/c^4 . \quad (3)$$

The measured scattering intensities I are related to the scattering efficiencies through[22]

$$I = [(1-R_i)(1-R_s)/(\alpha_i+\alpha_s)n_s^2]S , \quad (4)$$

where R_i and R_s are the reflectivities for incident and scattered radiation, α_i and α_s the corresponding absorption coefficients and n_s the reflective index of the scattered radiation (collection-angle correction). We measure at 1.92 eV $I_{\alpha\text{-Sn}}/I_{Si} = 0.04$. From this value and using the optical constants of α-Sn given in Ref. 14 and those of Si from Ref. 23, we find $S_{\alpha\text{-Sn}}/S_{Si} = 8.1$. With this value and the theoretical value of P for Si, Eqs. (1) and (2) yield $d^5_{3,0} = 18$ eV for α-Sn, somewhat smaller than the value expected from Fig. 3 (31 eV). A value of $d^5_{3,0} = 19$ eV, also smaller than that predicted by pseudopotential calculations ($d^5_{3,0} = 37$ eV) has been recently measured for GaAs.[24]

B. Second-order scattering

Figure 5(a) displays the first- and second-order Raman spectrum of α-Sn for a laser wavelength $\lambda = 7525$ Å(1.65 eV) at a power of 150 mW. The arrows indicate the two-phonon overtone critical points, as derived from Ref. 10.

Figure 5(b) shows the calculated density of two-phonon states taken from the work of Tubino *et al.*[12] In the latter work the valence-force potential method has been used to obtain phonon-dispersion curves fitting the experimental points of Ref. 10 (Fig. 6) and the calculations of $g(\omega)$ have been performed by a root sampling method using 5000 distinct $\vec{q}$'s in one irreducible element of the Brillouin zone ($\frac{1}{48}$ of the volume of the whole Brillouin zone).

There is a relatively good correspondence in peak positions between the two-phonon density of states and the second-order spectrum. In the acoustical region we were able to resolve only a structure at 108 cm^{-1}, which probably comes from overtone processes at W and/or Σ critical points.

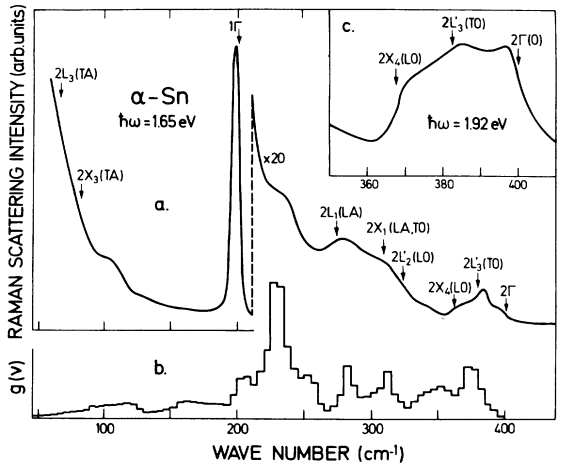

FIG. 5. Density of overtone two-phonon states of α-Sn (Ref. 12) compared with the second-order Raman scattering. Inset shows resonant enhancement of the 2Γ (O) scattering at 1.92 eV.

The structure above the first-order peak resembles the second-order spectra of Ge and Si. At 230 cm^{-1}, a shoulder corresponds to the strong peak in the two-phonon density of states. It should be mentioned that a peak at that energy was found

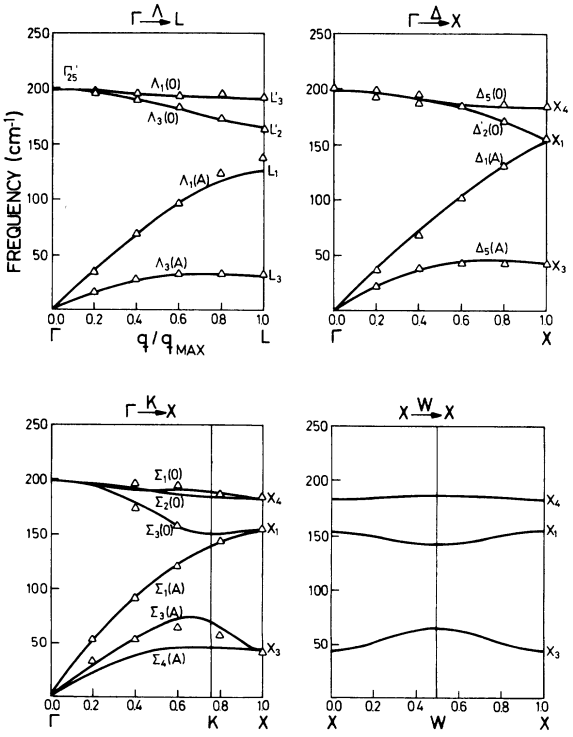

FIG. 6. Dispersion relations of α-Sn calculated in Ref. 12 (the labelling of the TO and LO modes at L given in this reference is incorrect. We have accordingly corrected it). Points are from neutron scattering.

also in the phonon spectrum derived from inelastic neutron scattering.[9] Basing ourselves on the dispersion curves of Fig. 6, we could tentatively assign this peak to phonon combinations $X_4(0) + X_3(A)$.

The broad structure between 265 and 330 cm^{-1} peaks at 280 and 315 cm^{-1}. The accuracy in determination of peak position is not higher than ± 5 cm^{-1}. Here the contributions could come both from overtone and combinations processes.

In the region between 360 and 400 cm^{-1} should lay the structure due to two-phonon overtone processes at the X, L, and Γ points. The position of $2L_3'$ (TO) peak was found to be 383 ± 2 cm^{-1}. Although the laser frequency is in the region of E_1 resonance, the 2Γ (TO) structure is less pronounced than for the cases of Ge and Si. The existence of the shoulder at the double frequency of the optical phonon at $\vec{q} = 0$ is most clearly seen at excitation with 6471 Å (1.92 eV) laser line, closer to the $E_1 + \Delta_1$ gap [Fig. 5(c)]. This 2Γ (O) structure has been attributed to iterated electron–one-phonon interaction which should resonate more strongly than the rest of the spectrum.[3,4]

C. Second-order resonance

In order to get some idea about the resonance behavior of the second-order spectrum, we have measured the first- and second-order RS spectra of α-Sn with three other laser lines, namely, 6471 Å(1.92 eV), 5017 Å(2.47 eV), and 4579 Å (2.71 eV). The intensities of the $2L_3'$ (TO) peaks were then normalized using the first-order resonance curve. The points estimated in this way are shown on Fig. 7.

In the scattering configuration used (no analyzer) all three components Γ_1, Γ_{12}, and Γ_{25}' of the Raman tensor are allowed. The Γ_1 component, which consists mainly of overtone scattering, contains only two-band terms. It should be proportional to $d\chi/d\omega$ and should peak near E_1, and $E_1 + \Delta_1$. The experimental points of Fig. 7 qualitatively follow such a dependence (dashed line). However, the higher value of the point at 1.65 eV indicate that the Γ_{12} and Γ_{25}' components which contain three-band terms, can not be neglected and a more precise description has to account for both two-band and three-band processes.

The different resonance curves for the first- and second-order RS cross sections in α-Sn could explain the high value of first- to second-order intensity ratio of Fig. 5(a). This ratio decreases strongly if one goes far from the resonance and becomes comparable with that of other diamond-like and zinc-blende semiconductors.

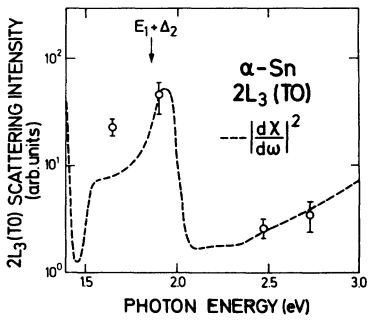

FIG. 7. Resonance of the scattering by 2TO (L) peak near $E_1 + \Delta_1$. Dashed curve corresponds to the theory for two band processes.

IV. CONCLUSIONS

The first- and second-order scattering due to phonons in α-Sn, and its resonance in the 1.5–3.5-eV region, has been investigated. The first-order scattering shows a resonance near the $E_1 + \Delta_1$ edge (1.8 eV) which can be interpreted in terms of three-band processes with a deformation potential $d_{3,0}^5$ (the two-band deformation potential $d_{1,0}^5$ is negligible). The first evidence for an E_2 resonance at around 3.5 eV in the one-phonon scattering of tetrahedral semiconductors has been obtained. This resonance, however, could not be quantitatively analyzed because of an insufficient number of experimental points. The two-phonon scattering has been analyzed in terms of critical points. It resonates mainly in the two-band electron–two-phonon interaction fashion expected for the Γ_1 component. Close to $E_1 + \Delta_1$, a more strongly resonant peak develops at the energy of 2Γ (O) phonons. Its behavior is similar to that found for Ge and Si, and thus can be interpreted as iterated scattering by electron–one-phonon interaction.

ACKNOWLEDGMENTS

We would like to thank W. Paul for supplying the α-Sn crystals, G. Güntherodt for carrying them from the U.S. to Germany under refrigeration, D. E. Aspnes for processing the χ^+ and χ^- used here, and G. Wolff for his invaluable technical assistance.

*Supported in part by the Alexander von Humboldt Foundation, on leave from the Faculty of Physics, Sofia University, Bulgaria.

†Supported in part by the Alexander von Humboldt Foundation, on leave from the Institute of Semiconductors of the Academy of Sciences of USSR, Novosibirsk, USSR.

[1]B. A. Weinstein and M. Cardona, Phys. Rev. B 7, 2545 (1973).

[2]M. A. Renucci, J. B. Renucci, and M. Cardona, Solid State Commun. 14, 1295 (1974).

[3]M. A. Renucci, J. B. Renucci, R. Zeyher, and M. Cardona, Phys. Rev. B 10, 4309 (1974).

[4]J. B. Renucci, R. N. Tyte, and M. Cardona, Phys. Rev. B 11, 3885 (1975).

[5]W. Dreybrodt, W. Richter, F. Cerdeira, and M. Cardona, Phys. Status Solidi B 60, 145 (1973).

[6]W. Kiefer, W. Richter, and M. Cardona, Phys. Rev. B 12, 2346 (1975).

[7]R. Loudon, Adv. Phys. 13, 423 (1964).

[8]See W. Richter, *Resonant RS in Semiconductors* (Springer, Berlin, 1975), Vol. 78, p. 121, and references therein.

[9]V. Myers, J. Phys. Chem. Solids 28, 2207 (1967).

[10]D. L. Price, J. M. Rowe, and R. M. Nicklow, Phys. Rev. B 3, 1268 (1971).

[11]C. J. Buchenauer, M. Cardona, and F. H. Pollak, Phys. Rev. B 3, 1243 (1971).

[12]R. Tubino, L. Piseri, and D. Zerbi, J. Chem. Phys. 56, 1022 (1972).

[13]P. Merlin and M. Iliev (unpublished).

[14]T. Hanyu, J. Phys. Soc. Jpn. 31, 1738 (1971).

[15]M. Cardona and P. McElroy, Solid State Commun. 4, 319 (1966).

[16]M. Cardona and D. L. Greenway, Phys. Rev. 125, 1291 (1961).

[17]R. Zeyher (unpublished).

[18]R. E. Lindquist and A. W. Ewald, Phys. Rev. 135, 191 (1964).

[19]D. E. Aspnes and M. Cardona (unpublished).

[20]K. L. Shaklee, J. E. Rowe, and M. Cardona, Phys. Rev. 174, 874 (1968).

[21]L. R. Swanson and A. A. Maradudin, Solid State Commun. 8, 859 (1970).

[22]R. Loudon, J. Phys. (Paris) 26, 677 (1965).

[23]H. R. Philipp, J. Appl. Phys. 43, 2835 (1972).

[24]R. Trommer and M. Cardona (unpublished).